Fuel 264 (2020) 116768

Contents lists available at ScienceDirect

Fuel

journal homepage: www.elsevier.com/locate/fuel

Full Length Article

Oxidation and pyrolysis of ammonia mixtures in model reactors

Maria Virginia Manna[a,b,*], Pino Sabia[b], Raffaele Ragucci[b], Mara de Joannon[b]

[a] DICMAPI-Università degli studi di Napoli Federico II, P.le Tecchio 80, 80125 Naples, Italy
[b] Istituto di Ricerche sulla Combustione-CNR, P.le Tecchio 80, 80125 Naples, Italy

ARTICLE INFO

Keywords:
Ammonia oxidation
Ammonia pyrolysis
Heterogeneous effects
Combustion

ABSTRACT

The present work was devoted to an experimental characterization of NH_3 oxidation and pyrolysis processes in model reactors. The oxidation tests were performed in a Jet Stirred Flow Reactor (JSFR) for stoichiometric ammonia/oxygen/argon and ammonia/oxygen/argon/water mixtures, as a function of mixture inlet temperature (T_{in}), at fixed pressure and residence time. Following, the behavior of ammonia/oxygen/argon mixture was analyzed in two tubular laminar flow reactors (LFRs) made of different materials (quartz and alumina), to evaluate potential surface heterogeneous effects.

Pyrolysis tests were performed in both the reference model reactors, by substituting oxygen with argon.

Experimental results realized in the JSFR allowed to identify three different kinetics regimes in ammonia oxidation: low (T_{in} < 1130 K), intermediate (1130 < T_{in} < 1250 K) and high temperatures (T_{in} > 1250 K). Surface heterogeneous reactions seemed to be negligible on ammonia reactivity and hydrogen profiles, but some effect could be observed on NO_x concentration in the low-intermediate temperature range. Experiments realized in presence of water suggested that such species may passivate the surface, minimizing heterogeneous effects.

Experimental tests realized in the LFRs confirmed these results, as hydrogen and oxygen profiles were independent of the reactor material, while NO_x concentrations exhibited significant changes. Experimental results suggested that heterogeneous reactions were more relevant under pyrolytic conditions.

Numerical simulations were performed with different kinetic mechanisms available in literature to value their capability to describe ammonia chemistry. None of them could accurately reproduce the experimental data for ammonia oxidation process, while they completely failed to predict ammonia pyrolysis features.

1. Introduction

The development of technologies for alternative energetic sources is a fundamental concern for the transition toward a new energetic scenario, which is able to ensure high efficiency in energy supply and low environmental impact [1]. The main issues to be faced regard the intrinsic intermittence and the seasonal variability of the renewable sources [2]. The technologies for the energy surplus storage are still inadequate and expensive with respect to the storage in the chemical bonds of molecules [3]. Furthermore, batteries have lower energy density and shorter discharge time (i.e. batteries) than chemicals [4]. For these reasons, combustion processes still play an important role in energy production but global warming acceleration and the request of alternatives to fossil fuels require to focus the attention on non-conventional fuels, which do not alter the natural carbon cycle [5]. Energy carriers include molecules derived from conventional or bio-derived fuels as well as molecules obtained by means of conventional processes to store the renewable sources energy surplus. Among these substances, carbon free compounds, i.e. hydrogen and ammonia, are recognized as promising alternative fuels, since they can be oxidized without CO_2 emissions. However, the implementation of a hydrogen-based energy production is not still realistic due to the difficulty concerning hydrogen storage and distributions [6]. Ammonia can be considered an interesting solution (as a hydrogen vector or as fuel itself) since an efficient ammonia transport network already exists [7]. However, NH_3 physical and chemical properties (flame velocity, low calorific value, minimum ignition temperature) and the high NO_x levels production in combustion processes could represent a limit for the application of ammonia as alternative fuel. For these reasons, a deeper understanding of NH_3 oxidation mechanism is necessary to identify optimal operating conditions and minimize NO_x emissions. The gas phase kinetic studies on the oxidation processes are frequently performed in shock tubes, premixed flames and continuous stirred tank reactors [8]. In particular, quartz Jet Stirred Flow Reactors (JSFRs) can be considered ideal to prevent surface effects, due to the quartz inactivity in the oxidation reactions. Nevertheless, the interpretation of data on the oxidation of ammonia in

* Corresponding author at: P.le Tecchio 80, 80125 Naples, Italy.
E-mail address: mariavirginia.manna@unina.it (M.V. Manna).

https://doi.org/10.1016/j.fuel.2019.116768
Received 21 June 2019; Received in revised form 25 November 2019; Accepted 26 November 2019
Available online 13 December 2019

quartz JSFR must be careful, as Glarborg et al. [9] suggest, because, due to slow ammonia homogeneous reactions, heterogeneous interaction with surfaces can be relevant, thus introducing uncertainties in the evaluation of the gas phase reactivity. Several works deal with the interaction between ammonia and solid surfaces [10–15]. Tsyganenko et al. [15] studied the formation of surface species arising from the adsorption of ammonia on oxide surfaces. They suggested that the way ammonia interacts with solid oxides depends on the temperature and on the presence of hydroxyl group on oxide surface. They mentioned three types of retention:

1. Formation of hydrogen-bonding between the nitrogen atom of ammonia and the hydrogen atom of the hydroxyl group on oxide surface;
2. Formation of hydrogen-bonding between the hydrogen atom of ammonia and the oxygen atom of the solid oxide;
3. Lewis interaction among ammonia and electron-deficient metal atom of the oxide.

The system temperature can boost the dehydroxylation of the material surface, thus influencing the type of surface interaction. Tsyganenko et al. [15] found different spectra of ammonia adsorbed on SiO_2 surfaces while heating the sample up to 700–800 °C. At higher temperatures, they observed the spectrum of surface NH_2 group, not revealed at low temperatures. They found analogues results studying the spectrum of ammonia adsorbed on Al_2O_3.

Glarborg et al. [9] studied the potential impact of these surface interactions on the thermal $DeNO_x$ process in a flow reactor. They described the heterogeneous decomposition of ammonia by a single-site ammonia adsorption step. They modeled the experimental NH_3 and NO profiles obtained by Hulgaard and Dam-Johansen [16] in a plug flow, with and without the surface chemistry. They claimed that heterogeneous reactions are negligible for the analyzed conditions, due to small reactor surface/volume (S/V) ratio [9,17]. In addition, Glarborg et al. argued that the presence of H_2O may inhibit the surface decomposition of ammonia because water can interact with solid oxides by both molecular and dissociative adsorptions depending on the temperature [18–20]. Kijlstra et al. [18] studied the effect of water in Selective Catalytic Reduction (SCR) processes, and they suggested that water can inhibit or deactivate both the catalyst and the γ–Al_2O_3 support reactivity.

Despite the literature is plenty of works dealing with ammonia heterogeneous chemistry on surfaces, for the most they are relative to SCR catalysts (i.e. metals and metals oxides, noble metals, zeolite), and few and sparse information are available for quartz or alumina surfaces, usually used as catalyst supports [15,18].

Given this framework, the goal of the present work is to present an experimental study on the NH_3 oxidation and pyrolysis in a JSFR, keeping in account the effects of the surface interactions on the processes. For this purpose, experimental tests with ammonia/oxygen mixtures diluted in Ar and Ar-H_2O were performed. Water was used to passivate the quartz surface, following literature suggestions [9,17–20].

Furthermore, the analyses proceeded throughout experimental tests in a quartz and in an alumina tubular laminar flow reactors (LFR) to value the heterogeneous effects with different materials.

In addition, numerical simulations were performed with different detailed kinetic mechanisms to value their capability to predict experimental data and understand the ammonia oxidation and pyrolysis controlling chemistry, relevant for the investigated operative conditions.

2. Experimental and numerical methods

Experimental tests were realized in a quartz Jet Stirred Flow Reactor (JSFR) and in two tubular Laminar Flow Reactors (LFR) made of different materials (quartz and alumina).

The JSFR experimental facility comprises several mass flow controllers for gas supply to the reactor (supplied by BronkHorst High Tech). For water supply, the system is equipped with an evaporator system (CEM BronkHorst Hith Tech) and a liquid mass flow controller. They are interfaced with a PC and controlled by a dedicated program developed in Labview. The core of the system is a fused silica spherical JSFR reactor (113 cm^3, ID equal to 6 cm).

The detailed description of the experimental facility and of the reactor is reported elsewhere [21].

The experiments were performed at atmospheric pressure and fixed residence time (τ), as a function of the mixture inlet temperature (T_{in}). The oxidation process was analyzed for a NH_3/O_2 stoichiometric mixture. The equivalence ratio (Φ) was defined on the basis of the reaction $4NH_3 + 3O_2 \rightarrow 2\ N_2 + 6H_2O$, according to this equation:

$$\phi = \frac{(NH_3/O_2)}{(NH_3/O_2)_{stoich}} = \frac{3}{4}(NH_3/O_2).$$

Mixtures were diluted in Ar and in Ar-H_2O. Ar was chosen as diluent because it allowed to investigate the formation of N_2 and NO coming exclusively from NH_3, while water was used as an attempt to passivate the reactor surface.

The experimental conditions exploited in the JSFR are summarized in Table 1.

The experiments were conducted with such a relatively low dilution level to properly characterize the catalytic effect of surfaces, by measuring H_2 and N_2 with reasonable concentration level (compatible with instruments sensitivity).

Additional tests were executed at fixed temperatures and residence time with a higher percentage of H_2O (3.4%) to analyze the effectiveness of the surface passivation.

To monitor the temperature changes during gaseous reactions, an unshielded thermocouple type R (0.1 mm tip size) made in-house was used. It has a fast response time (less than 30 ms) and a precision of ± 0.25%.

The two laminar flow reactors (LFR) are 1 m long with an ID equal to 0.008 m, and an OD of 0.012 m. The mixture velocity was fixed equal to 3 m/s to ensure $\left(\frac{D}{uL}\right) < 0.01$ to neglect dispersion effects and assume a plug flow reactor behavior [22].

The reactors are displaced symmetrically within two semi-cylindrical electrically heated ceramic fiber ovens with a heating length of 0.6 m. The temperature within the oven is monitored by five thermocouples (type N, with a precision of ± 0.75%) equi-distributed along the height of the heated part of reactors and located close to their external surface. Air is insufflated within the ovens to homogenize the temperature, thus resulting in a maximum difference between the inlet and outlet of the LFRs of about 10 K under non-reactive conditions.

The averaged value of the five thermocouples was chosen as the reference temperature (T_{ref}) for the experimental tests. Another thermocouple (type N) is positioned inside each reactor at the end of the heated part as indicator of system reactivity.

Experimental tests were realized for mixtures highly diluted in Ar at atmospheric pressure and fixed velocity. The experimental conditions are summarized in Table 2.

It must be underlined that the S/V ratio for the LFRs is approximatively 5 times greater than the one of the JSFR, thus the effect of

Table 1
Experimental operative conditions for the oxidation and pyrolysis tests in JSFR.

Conditions	Oxidation	Pyrolysis
Inlet temperature (T_{in})	900–1350 K	1000–1350 K
Equivalence ratio (Φ)	1	1
Residence time (τ)	0.25 s	0.25 s
Pressure	1.2 atm	1.2 atm
Diluent (d)	86% Ar	92% Ar
	84.3% Ar – 1.7% H_2O	90.3%–1.7% H_2O

Table 2
Experimental operative conditions for tests in LFRs.

Conditions	Oxidation and Pyrolysis
Inlet temperature (T_{in})	900–1350 K
Equivalence ratio (Φ)	1
Diluent (oxidation) (d)	86% Ar
Diluent (pyrolysis) (d)	92% Ar
Velocity	3 m/s
Pressure	1.2 atm

heterogeneous reactions is expected to be enhanced.

For all the reactors, the exit gases were cooled down by means of a heat exchanger installed at the reactor outlet to quench the oxidation reactions in the sampling line. The exhaust gases temperature is maintained at about 80 °C by means of a heating system to prevent water condensation (considering the water maximum vapor pressure in the exhausted flow) and ammonia solubilization. Water is then removed by a silica gel trap prior chemical analyses (data are reported on a dry basis).

The outlet species (H_2, N_2, O_2) were analyzed by a gas-chromatograph (Agilent 3000). NO_x and O_2 concentration were also detected using an online analyzer (TESTO 350).

The maximum relative errors in mole fractions of O_2 and H_2 species are around ± 3%. The estimated error for NO_x emissions is ± 2 ppm in the range of 0–99.9 ppm, and ± 5% in the range of 100–500 ppm.

The JSFR experimental results were simulated using the PSR code of Chemkin PRO [23] package.

Each test was repeated at least three times and, to value the reproducibility of data, the same operative conditions were replicated in different days.

The system was modeled as "non-adiabatic" with a global heat transfer coefficient equal to 3.5×10^{-3} cal/cm^2 s K. The heat transfer coefficient evaluation is provided in the supplementary materials.

Four different detailed gas-phase chemical kinetic models were used. Authors, numbers of species and reactions are reported in Table 3.

The Konnov et al. [24] model is a complete H/N/O mechanism tested for decomposition, oxidation, ignition, and flame structure of ammonia. It is an integral part of the model developed for the combustion of small hydrocarbons (C_1–C_3).

The Glarborg et al. [25] model is developed for modeling nitrogen chemistry in combustion processes. It was validated using experimental data taken in model reactors (tubular flow reactors and batch reactors) for light hydrocarbons (CH_4) and ammonia oxidation.

The mechanism developed by Song et al. [26] derives from a previous model by Klippenstein et al. [28]. It was tuned to predict experimental data collected in laminar plug flow quartz and alumina reactors at high pressure (30–100 bar).

The Nakamura et al. model [27] was validated on the basis of experimental tests in a micro flow reactor with controlled temperature profiles, at low temperatures and for different equivalence ratios. Their model was updated mainly for the N_2H_x chemistry because the reactions that involve N_2H_x species were expected to be significant in the considered temperature range.

Hereafter, the kinetic models will be identified in the manuscript as "Konnov", "Glarborg", "Song" and "Nakamura".

Table 3
Kinetic mechanisms and details.

Kinetic mechanism	Number of reactions	Number of species
Konnov [24]	286	36
Glarborg et al. [25]	1397	151
Song et al. [26]	204	34
Nakamura et al. [27]	232	38

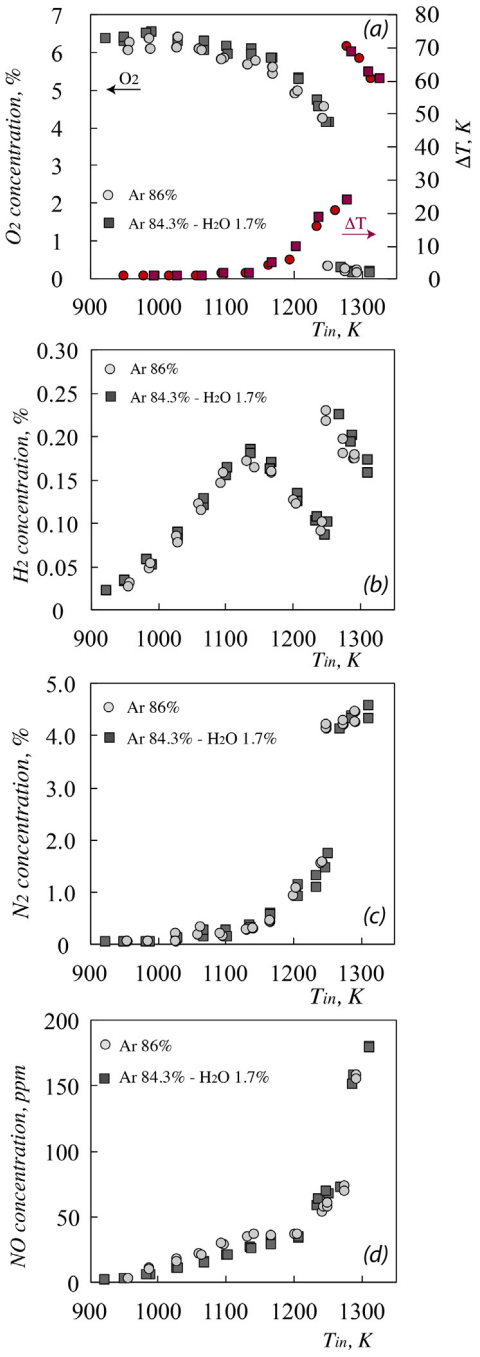

Fig. 1. ΔT, O_2, H_2, N_2, NO experimental profiles as a function of T_{in}, for the oxidation of stoichiometric $NH_3/O_2/Ar$ (d = 86%) and $NH_3/O_2/Ar/H_2O$ (d = 84.3% Ar-1.7% H_2O) mixtures, at fixed p = 1.2 atm and τ = 0.25 s, in JSFR. (For interpretation of the references to colour in this figure legend, the reader is referred to the web version of this article.)

3. Results and discussions

3.1. Oxidation in JSFR

The experimental results on the NH_3 oxidation are presented in this section. In particular, Fig. 1 shows the O_2, H_2, N_2, NO experimental profiles as a function of T_{in}, for stoichiometric $NH_3/O_2/Ar$ and $NH_3/O_2/Ar/H_2O$ mixtures.

For both the mixtures, the O_2 conversion (Fig. 1a, grey symbols) is negligible for $T_{in} < 1200$ K, then it starts to increase with T_{in}, and for $T_{in} > 1250$ K it is complete. The temperature profile (Fig. 1a, red

symbols) is consistent with the O_2 trend. The maximum measured temperature increase is about 70 K at T_{in} = 1300 K, remarkably lower than the calculated one for adiabatic condition ($T_{adiabatic}$ = 670 K), due to the heat exchange phenomena.

Fig. 1b is relative to the H_2 concentration. It is possible to see that for both the mixtures, H_2 concentration increases with T_{in} up to a relative maximum value of about 0.18% for T_{in} = 1130 K, then for 1130 < T_{in} < 1250 K it decreases down to the minimum (0.085%). For T_{in} = 1250 K, it reaches its maximum concentration then it is consumed.

Independently of surface effects, the H_2 non-monotonous trends suggest the existence of three different kinetic regimes in the ammonia oxidation: low (T_{in} < 1130 K), intermediate (1130 < T_{in} < 1250 K) and high temperatures (T_{in} > 1250 K).

The N_2 concentration, coming from ammonia reactions, increases monotonically as a function of the inlet temperature (Fig. 1c).

The similarity of the key species profiles for the two analyzed mixtures suggests that NH_3 reactivity is not affected by surface interactions, for the operative conditions here investigated (mixture composition, averaged residence time and JSFR surface/volume ratio).

On the contrary, small differences can be observed for the NO profiles (Fig. 1d). For the mixture without H_2O, NO concentration increases as a function of the temperature for T_{in} < 1130 K, then it is almost constant for 1130 < T_{in} < 1250 K. For higher temperatures, it abruptly rises up to 160 ppm.

In presence of H_2O, NO concentration monotonically increases as a function of T_{in}. In general, values are very similar for both the mixtures in the all temperature range investigated, with small differences in the intermediate temperature range. As such, NO are slightly greater for the Ar diluted mixture with respect to the Ar-H_2O diluted one. However, these differences consist of no more than 5–6 ppm (value close to the instrument detection limit) and are restricted to the intermediate temperature range.

3.2. Pyrolysis in JSFR

The main results for the pyrolysis of NH_3/Ar and NH_3/Ar/H_2O mixtures as a function of T_{in} are reported in Fig. 2.

For both the mixtures, H_2 (Fig. 2a) and N_2 (Fig. 2b) profiles suggest that the decomposition starts at T_{in} > 1120 K. In presence of H_2O the amount of H_2 and N_2 results to be lower. The more the temperature increases, the more these differences become important.

These data suggest that heterogeneous reaction affects NH_3 decomposition more than for NH_3 oxidation, because of slower or comparable pyrolytic characteristic kinetic time with respect to heterogeneous ones. In the case of ammonia oxidation, such effects are maybe reduced because oxidation characteristic times are shorter than heterogeneous ones.

The effectiveness of the water surface passivation was evaluated for two fixed temperatures (T_{in} = 1220, 1270 K) by changing the amount of H_2O in initial composition (Fig. 3).

Results show that an increase of the H_2O concentration does not further reduce H_2 and N_2 concentration. This may suggest that surfaces could be considered passivated when the H_2O content is set equal to 1.7%. Thus, even if it is not a straightforward proof that steam passivates the surface, such results are comforting, and seem to suggest that at least steam minimizes these heterogeneous effects.

In addition, this behavior is not likely to be ascribable to homogeneous kinetic effects related to the water decomposition, since it would occur in presence of O radicals according to reaction $H_2O + O = OH + OH$ [21,29]. In these operative conditions, no oxygen is fed to the system, thus no O radicals would be present in the system.

As a further consideration, the direct comparison between N_2 profiles (if considered as inert species since very low NO_x emissions) under oxidative (from Fig. 1) and pyrolytic (from Fig. 2) conditions, for the mixtures partially diluted in water, shows that they overlap, thus supporting the potentiality of water to passivate the surface (as reported in Fig. 4).

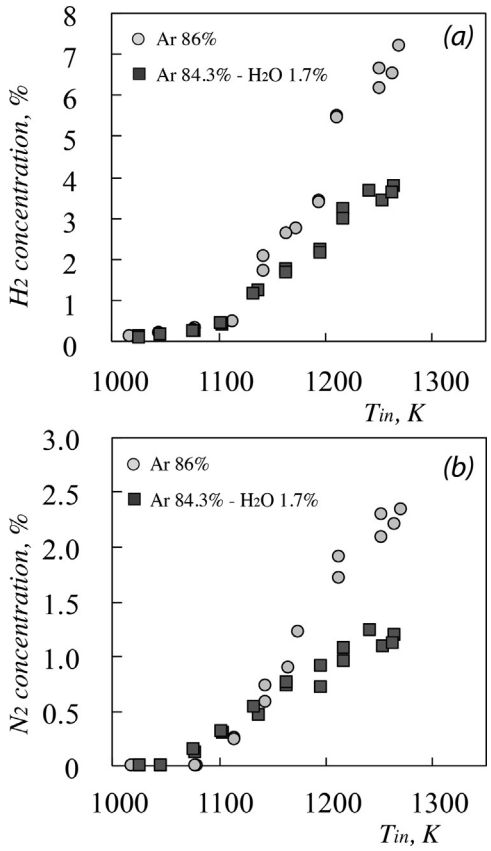

Fig. 2. H_2 and N_2 experimental profiles as a function of T_{in}, for the pyrolysis of NH_3/Ar (d = 92%) and NH_3/Ar/H_2O (d = 90.3% Ar-1.7% H_2O) mixtures, at fixed p = 1.2 atm and τ = 0.25 s, in JSFR.

3.3. Oxidation in laminar flow reactors

The experimental results presented in Fig. 5 refer to the oxidation of a stoichiometric NH_3/O_2/Ar mixture in two LFRs.

Given the symmetry of the system, as reported in paragraph 2, the two tubular reactors can be considered to work in the same operative conditions (as verified by the temperature measured by the two thermocouples positioned internally at the end of the two reactors).

The influence of the materials is evaluated by a comparison of key species as a function of a reference temperature (T_{ref}). It is defined as the averaged value of five thermocouples equi-displaced along the external wall of the tubular flow reactors. For this reason, T_{ref} is not representative of the temperature within the reactors.

O_2 profiles (Fig. 5a) are very similar for both reactors. Its concentration remains equal to the inlet one up to 1200 K, then it decreases to 0. Similarly, H_2 profiles (Fig. 5b) are approximatively coincident for both reactors: for T_{ref} < 1120 K H_2 concentration is equal to zero, then, for higher T_{ref} it increases.

In the quartz reactor, for T_{ref} < 960 K NO concentration (Fig. 5c) increases until a relative maximum at around 30 ppm. For 960 < T_{ref} < 1250 K NO profile decreases down to 10 ppm, while for the higher temperatures, NO concentration abruptly rises to 1720 ppm.

Within the alumina reactor a similar NO trend can be observed. For T_{ref} < 960 K, NO concentration increases as a function of the temperature, then, for an intermediate temperature range (960 < T_{ref} < 1100 K) it decreases down to 40 ppm and at higher temperatures (T_{ref} > 1100 K) it increases again to a maximum

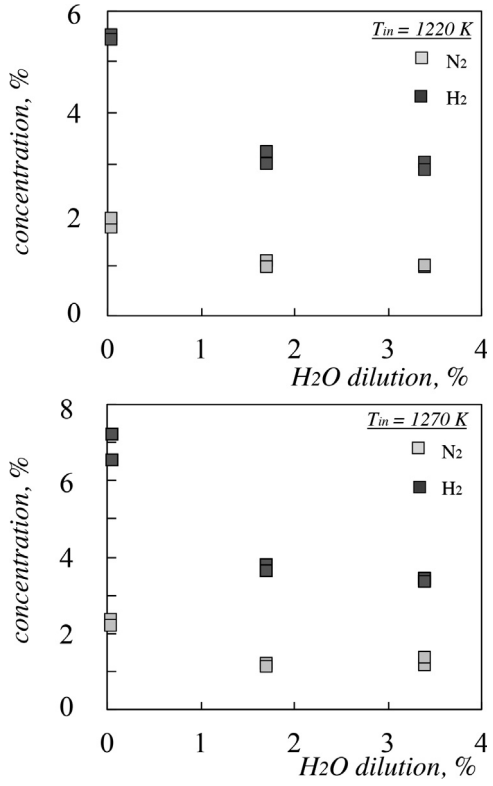

Fig. 3. H_2 and N_2 concentrations as a function of H_2O content for the pyrolysis of $NH_3/Ar/H_2O$ (overall d = 92%) mixtures, at fixed temperatures (T_{in} = 1220, 1270 K), p = 1.2 atm and τ = 0.25 s, in JSFR.

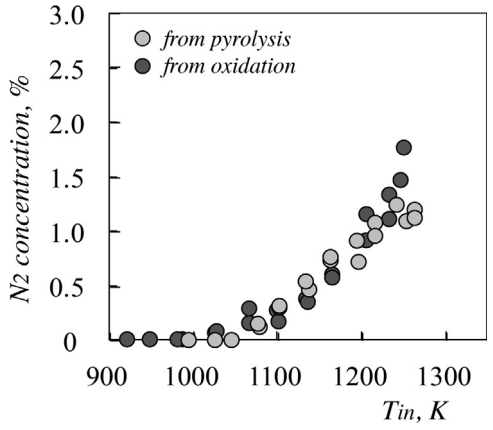

Fig. 4. Comparison between N_2 profiles from ammonia oxidation (d = 86%, ϕ = 1.0, p = 1.2 atm, τ = 0.21 s) and ammonia pyrolysis (d = 92%, p = 1.2 atm, τ = 0.21 s).

detected value of about 1800 ppm.

These results confirm the ones obtained in the JSFR. In fact, the O_2 and H_2 concentrations plotted with respect to T_{ref} are independent of the material, because they show the same trends and values for both the reactors, while NO profiles exhibit some different trends within the low-intermediate temperature regime. At higher temperatures, NO concentrations overlap, since NH_3 homogeneous reactions become relatively fast, thus heterogeneous reactions are less important.

The surface effect on the NO profiles are enhanced in the LFRs with respect to the JSFR, due to the greater S/V ratio. Additionally, the differences between the NO concentrations for the alumina and quartz reactors could be ascribed also to the different acidic properties of the materials [15].

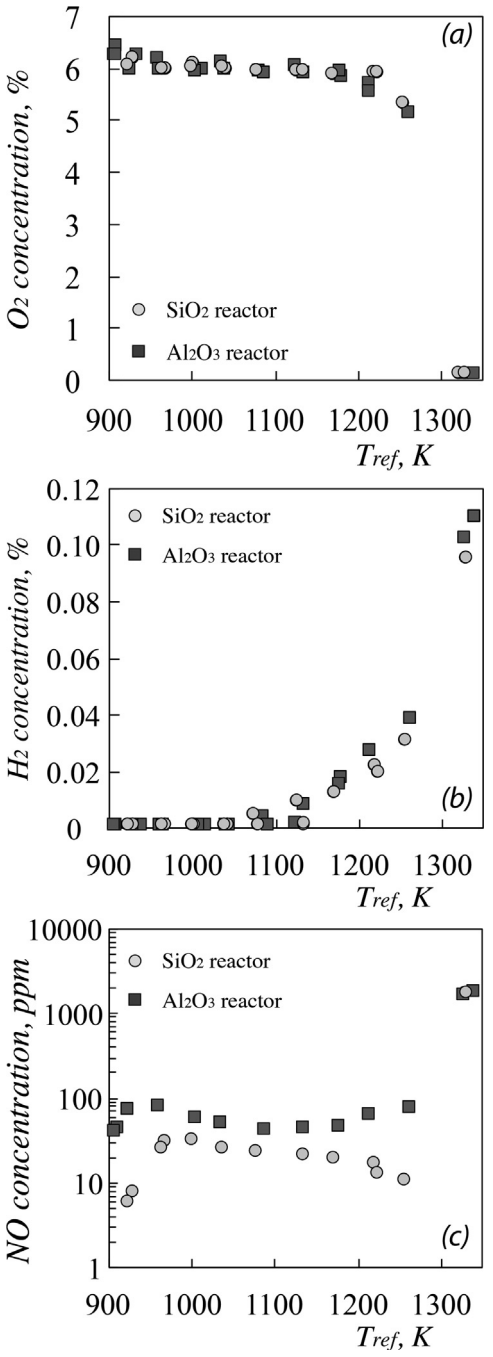

Fig. 5. O_2, H_2, NO experimental profiles as a function of T_{ref}, for the oxidation of stoichiometric $NH_3/O_2/Ar$ (d = 86%) mixture at atmospheric pressure and v = 3 m/s, in LFRs.

3.4. Pyrolysis in laminar flow reactors

Further tests were performed, analogously to the JSFR, for the NH_3 pyrolysis in LFRs. Results are reported in Fig. 6.

For these operative conditions, the detected species profiles exhibit significant differences depending on the material. H_2 (Fig. 6a) and N_2 (Fig. 6b) trends suggest that the NH_3 conversion starts at around T_{ref} = 1100 K for both the reactors and the decomposition is enhanced increasing the temperature. The higher H_2 and N_2 concentrations found for the alumina reactor, with respect to the fused silica one, highlight the strong impact of surface reactions on the ammonia thermal decomposition.

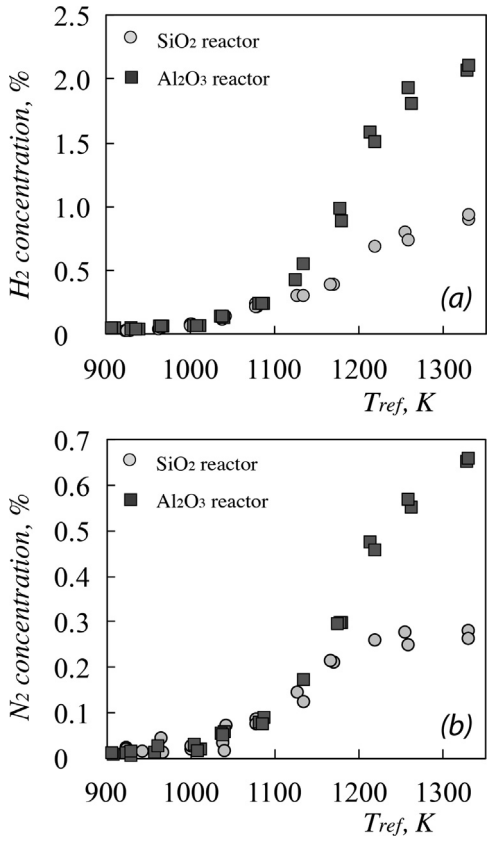

Fig. 6. H_2 and N_2 experimental profiles as a function of T_{ref}, for the pyrolysis of NH_3/Ar (d = 92%) mixture at atmospheric pressure and v = 3 m/s, in LFRs.

3.5. Numerical results

The experimental conditions performed in JSFR were simulated by the PSR code of CHEMKIN PRO [23], using the four kinetic mechanisms previously described. Simulations were performed for both the oxidative and pyrolytic conditions in order to value the capability of detailed kinetic schemes to reproduce the experimental data reported in this manuscript.

In this context, it is worth highlighting that the data obtained with the LFRs are not easy to model, because T_{ref} is not indicative of the real thermal state of the reactive mixtures. Thus, the data, previously reported give important information relatively to the interaction of ammonia homogeneous/heterogeneous chemistry with different materials, but they cannot be straightforwardly used for modeling activities. For this reason, simulations were performed considering the data from the JSFR.

The experimental data simulated in this section are relative to mixtures with small amount of water to ideally neglect surface effects, as previously pointed out.

The comparison among experimental and numerical results for ammonia oxidation is reported in Fig. 7.

As shown in Fig. 7, "Nakamura" and "Konnov" kinetic mechanisms predict a higher reactivity at low temperatures with respect to the experimental data and the existence of dynamic behaviors (temperature and species concentration oscillations, identified in the figure by dashed lines) at intermediate ones. In particular, "Nakamura" dynamic region extends in the temperature range 1120 < T_{in} < 1300 K while "Konnov" one lays in the temperature range 1110 < T_{in} < 1300 K.

"Song" and "Glarborg" mechanisms suggest no reactivity at low-intermediate temperatures. Additionally, "Glarborg" scheme predicts dynamic regimes in a very small temperature range (1200 < T_{in} < 1270 K).

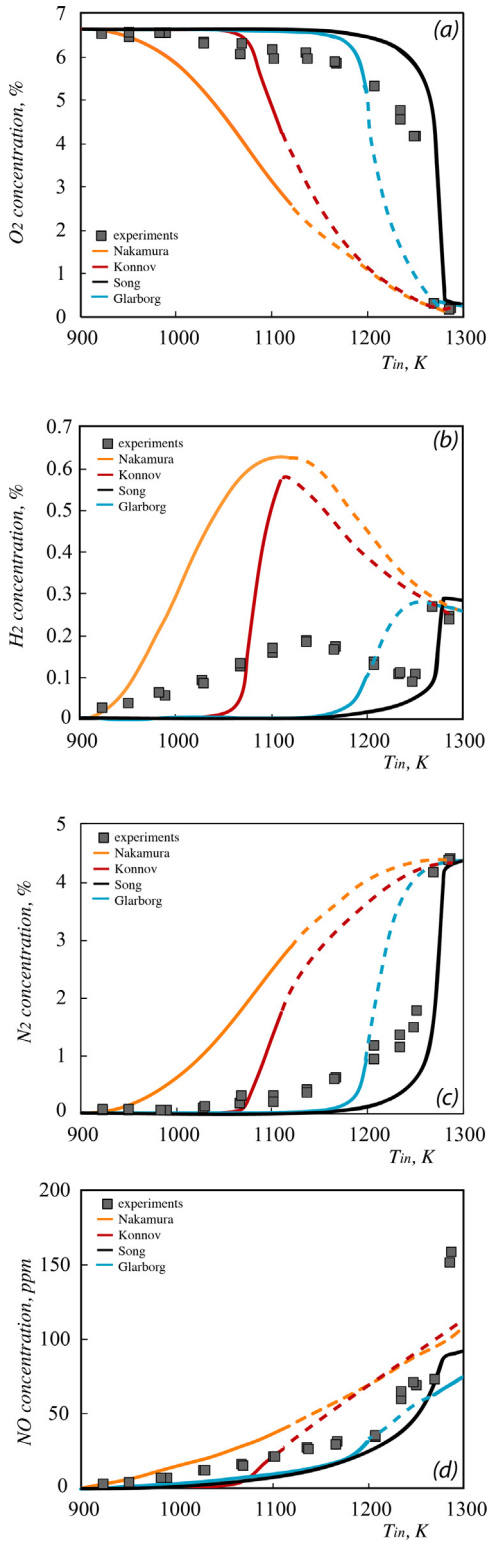

Fig. 7. Experimental and numerical species profiles for the oxidation of the stoichiometric $NH_3/O_2/Ar/H_2O$ mixture (d = 84.7% Ar – 1.7% H_2O), at fixed p = 1.2 atm and τ = 0.25 s, in JSFR.

"Nakamura" model is able to predict the H_2 experimental trend (Fig. 7b) at low temperatures, outside the dynamic-behavior region, but values are relatively overestimated.

"Song" and "Glarborg" schemes reproduce the experimental data at high temperatures, while the others still suggest the occurrence of dynamic behaviors. The experimental NO profile (Fig. 7d) is not properly

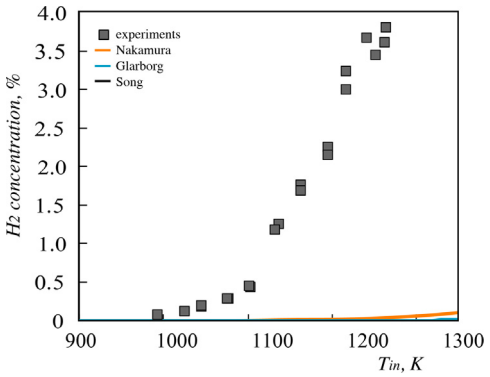

Fig. 8. Experimental and numerical H_2 profiles for NH_3 pyrolysis diluted to 92% in Ar, at fixed p = 1.2 atm, T_{in} = 900–1300 K and τ = 0.25 s, in JSFR.

reproduced by any considered schemes.

In general, it is worth highlighting that some kinetic schemes well predict O_2, H_2 and N_2 at high temperatures, thus suggesting that for these operative conditions the main problems come from the modeling of low-intermediate temperatures, where, regardless the matching with experimental data, all the models predict different species concentration trends and combustion regimes.

On the basis of numerical results, further experimental tests were carried on (changing residence time, dilution level, equivalence ratio and diluent species) in order to exploit the possibility to detect instabilities or multiple steady states, as suggested by the models. In the investigated operative conditions, such phenomenologies were not identified.

The agreement between experimental and numerical profiles is worse for the pyrolysis process. The comparison is shown in Fig. 8.

H_2 and N_2 numerical profiles obtained by "Glarborg" and "Song" mechanisms are almost zero in the entire investigated temperature range, while "Nakamura" model shows a slight NH_3 decomposition for T_{in} > 1200 K even though the species concentrations are remarkably lower with respect to the experimental values. "Konnov" numerical results are not reported since the CHEMIKIN PSR code gives convergence problems when this model is executed.

3.6. Numerical study on the NH_3 pyrolysis

Reaction rate and sensitivity analyses were performed for both oxidative and pyrolytic conditions in order to highlight the controlling chemistry of these processes.

Results obtained for the NH_3 oxidation are very complex, due to the different mechanism prediction and combustion regimes, and, to some extent, are mechanism-dependent. For the sake of briefness such analyses will be reported in another paper were simulations were extended also to further experimental tests realized diluting the reference mixtures in N_2.

Herein, the attention is focused to the pyrolytic conditions, because they represent a critical issue with strong implication also for the low-intermediate temperatures, as suggested but several scientific works. In fact, experimental evidences from several facilities show that the ammonia pyrolysis occurs at temperatures relatively lower with respect to the predicted ones, in agreement with results presented in this manuscript.

Monnery et al. [30] performed ammonia pyrolysis tests in a tubular quartz reactor for NH_3/Ar mixtures by changing NH_3 concentration from 0.5 to 2%. They found that at 1123 K ammonia conversion is around 3–4% for a mixture residence time equal to 0.18 s and 5–6% increasing the residence time to 0.4 s. These results are compatible with the ones obtained in the quartz LFR reported in the paragraph 3.4, as at T_{ref} = 1120 K and residence time equal to 0.2 s, the measured NH_3 conversion is around 5%.

In addition, Rahinov et al. [14] evaluated the decomposition of ammonia in a quartz tubular reactor. Quartz surface was passivated with ammonia. They found out that NH_2 is formed via gas-phase ammonia decomposition at 950 K, thus indicated the onset of NH_3 pyrolysis reactions.

Kobayashi et al. [31] presented an overview of available kinetic mechanisms of ammonia oxidation and fuel NOx. In particular, they analyzed the work by Miller et al. [32] and highlighted that their kinetic model was able to predict the experimental data for fuel lean flames under low pressure (20–50 Torr), but failed to predict data for stoichiometric and fuel rich conditions. They suggested that the ammonia pyrolysis reaction rates are strongly underestimated in the kinetic mechanism with strict consequences also for ammonia oxidation prediction.

This aspect is even more evident for the prediction of ammonia ignition delay time. Mathieu and Petersen [33] stressed how their model and Klippenstein et al.'s mechanism [28] differ in prediction of ignition delay times due to the different intermediate-sensitivity reactions and, particularly, they remarked the differences in the pyrolysis reactions (that involve NH_2 and N_2H_2 without involvement or molecular or atomic oxygen).

In order to investigate the controlling chemistry proposed by each model for ammonia pyrolysis, further numerical analyses were performed, extending the temperature range up to 2000 K, where higher ammonia conversion is expected to occur. The results are reported in Fig. 9.

"Konnov" model prediction is not reported for numerical convergence problems, as previously declared.

For all the mechanisms, the predicted onset of reactivity is shifted to higher temperatures with respect to the experimental data, even if the H_2 concentration trend is similar.

Key species sensitivity analyses were realized at T_{in} = 2000 K, where H_2 concentrations were equal for all the mechanisms.

The bar diagrams (Fig. 10) show the maximum values of the sensitivity coefficients with respect to the temperature for the main reactions involved in H_2 and N_2 formation, according to the considered models.

The sensitivity analysis suggests that for "Song" and "Glarborg" models, H_2 and N_2 exhibit high sensitivity to the same reactions. In particular, the maximum positive sensitivity occurs for reactions: $NH_3(+M) = NH_2 + H(+M)$, $NH_2 + NH_2 = N_2H_2 + H_2$, $N_2H_2 + M = NNH + H + M$.

This set of reactions is different for the "Nakamura" scheme. In this case, the maximum positive sensitivity values for H_2 and N_2 occur for reactions:

$N_2H_2 = NNH + H$, $N_2H_3 = N_2H_2 + H$, $NH_3 + NH_2 = N_2H_3 + H_2$.

A similar reactions set was identified as important also for lower temperatures (reported in Supplementary Materials), relevant for the

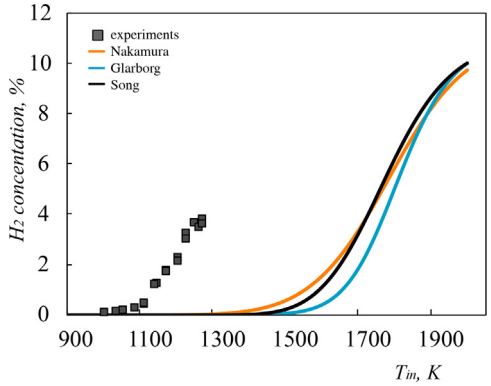

Fig. 9. Experimental and numerical H_2 profiles for NH_3 pyrolysis diluted to 92% in Ar, at fixed p = 1.2 atm, T_{in} = 900–2000 K and τ = 0.25 s, in JSFR.

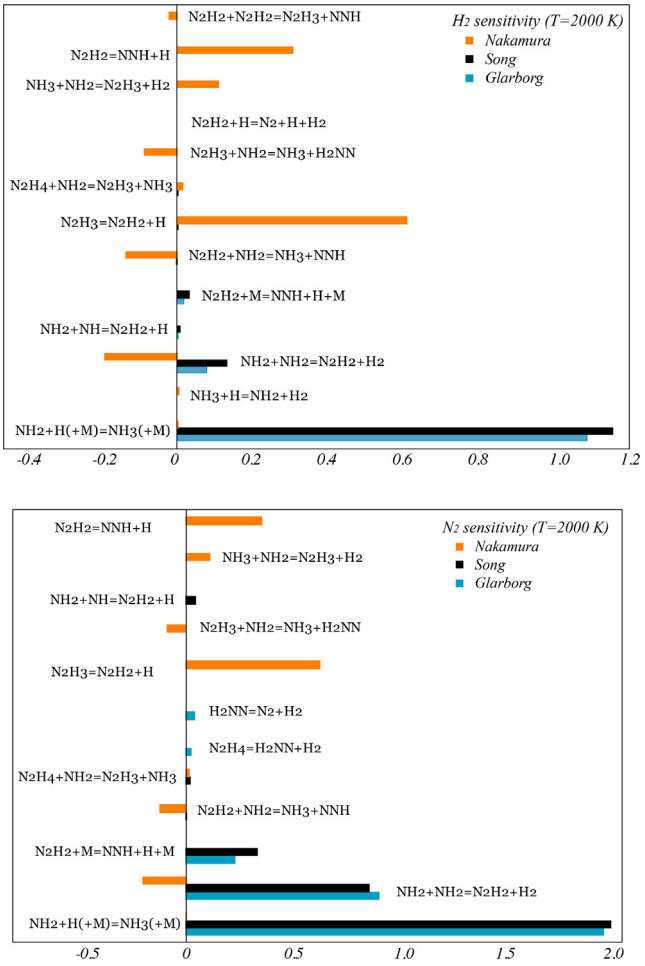

Fig. 10. Sensitivity analyses for NH_3 pyrolysis for T_{in} equal to 2000 K.

conditions exploited in this manuscript, thus suggesting the generality of these results.

The main reaction pathways were identified by means of flux diagrams. For the sake of briefness, the results obtained by "Song" mechanism were not reported, since they are similar to the ones obtained by "Glarborg" model (as also suggested by the sensitivity analysis).

In the flux diagrams (Figs. 11 and 12), the order of magnitude of all the reaction rates is 1E-1 and values reported in round brackets represent the multiplying factor. Arrows thickness is proportional to the reaction rate values.

Referring to "Glarborg" model (Fig. 11), NH_3 decomposes to NH_2 according to the reactions: $NH_3 + H = NH_2 + H_2$ and $NH_3 + H + M = NH_2 + H + M$. NH_2 is directly converted to N_2H_2 ($NH_2 + NH_2 = N_2H_2 + H_2$) or is dehydrogenated to NH ($NH_2 + H = NH + H$) and, subsequently, NH reacts with NH_2 to produce N_2H_2. N_2H_2 mainly isomerizes to H_2NN, which, in turn, decomposes to N_2 and H_2. Alternatively, N_2H_2 is dehydrogenated to NNH, which decomposes to N_2.

The analysis of the flux diagram obtained by "Nakamura" model (Fig. 12) suggests similar reaction pathways.

The main difference among the two mechanisms lays in the description of N_2H_2 consumption reactions. In particular, "Nakamura" model does not involve H_2NN, since N_2H_2 reacts with H to produce NNH and H_2.

Disregard the differences between the description of ammonia pyrolysis, the agreement with experimental data is not satisfactory. Beyond the occurrence of material catalytic effects, this aspect is well supported by literature evidences. Therefore, the comprehension of this chemistry seems to be prohibitive at the moment. This aspect would require a peculiar attention, also because strictly connected with the ammonia oxidation kinetics.

4. Conclusions

The present work describes the main features of the oxidation and thermal pyrolysis of a highly diluted stoichiometric $NH_3/O_2/Ar$ and NH_3/Ar mixtures in a quartz jet stirred flow reactor as a function of the inlet temperature (900–1350 K), at environmental pressure.

The H_2 and N_2 profiles obtained during the experimental tests suggest the existence of three different kinetic regimes for the ammonia oxidation: low ($T_{in} < 1130$ K), intermediate ($1130 < T_{in} < 1250$ K) and high temperatures ($T_{in} > 1250$ K).

Particular focus is paid on the interpretation of data at low-intermediate temperatures, where heterogeneous reactions on quartz surface are expected to affect ammonia chemistry. The experimental tests were repeated with small amount of steam (1.7%) used as surface passivating agent.

In addition, experimental tests were replicated also in a quartz and in an alumina tubular flow reactors to value the chemical heterogeneous interactions with different materials.

In the oxidation tests run in the JSFR, similar trends of main species profiles as a function of the mixture inlet temperature obtained with and without water suggest that NH_3 reactivity is likely to not be affected by surface interactions. On the contrary, heterogeneous reactions seem to partially reduce NO_x species in the low-intermediate temperature range.

For the pyrolysis tests run in the JSFR, the difference between

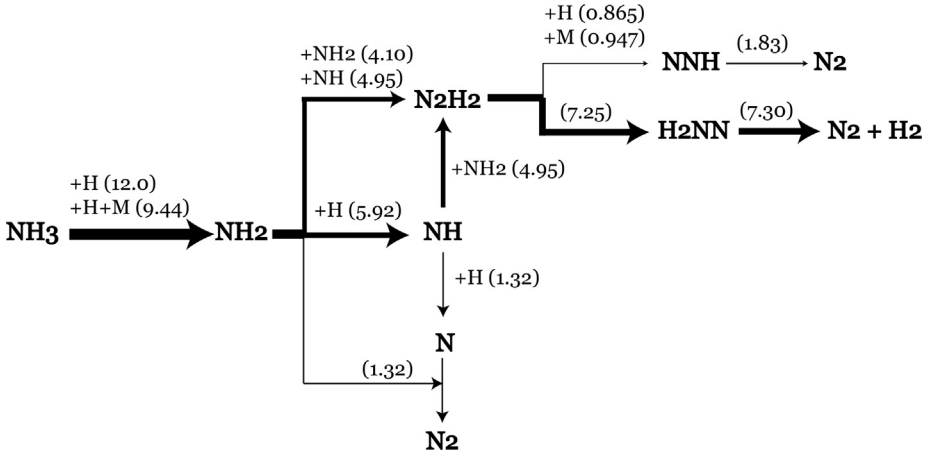

Fig. 11. Main reaction paths in NH_3 pyrolysis according to "Glarborg" mechanism, at $T_{in} = 2000$ K.

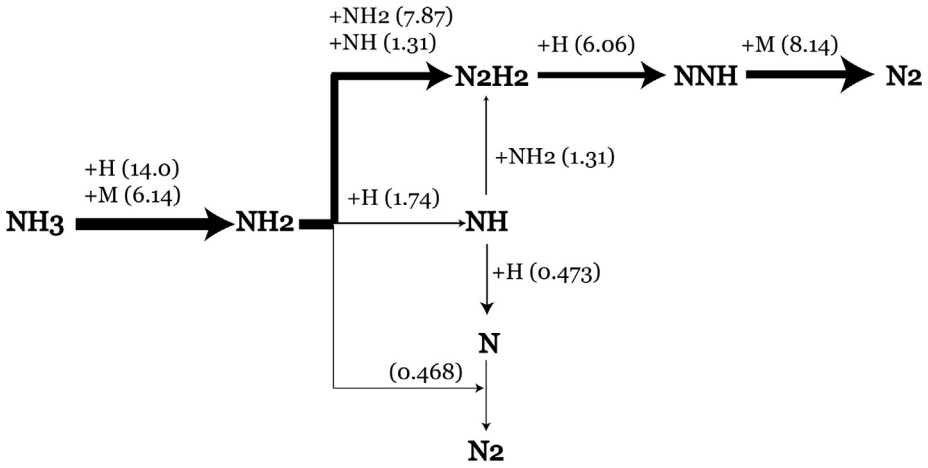

Fig. 12. Main reaction paths in NH_3 pyrolysis according to "Nakamura" mechanism, at T_{in} = 2000 K.

results obtained with or without water suggest that heterogeneous reactions are more effective, maybe due to the longer pyrolytic homogeneous characteristic times with respect to the heterogeneous ones.

Further experimental campaigns in two laminar flow reactors (quartz and alumina) endorse the results obtained in the JSFR. Relatively to ammonia oxidation tests, O_2 and H_2 concentrations are independent of the material, instead the NO profiles exhibit similar non-monotonous trends, with higher values for the alumina reactors at low-intermediate temperatures. For the pyrolytic conditions, H_2 and N_2 profiles are significantly different and higher values are detected for the alumina reactor, suggesting a stronger heterogeneous effect of such a material. In general, the LFRs are expected to be more effective as catalyzers with respect to the JSFR also because of a greater S/V ratio.

The experimental conditions performed in JSFR were simulated using four different kinetic mechanisms. The models are not able to accurately predict the experimental trends for the low-intermediate temperature ranges. In particular, all the considered models predict different trends for low-intermediate temperatures. Three of them suggest also the existence of dynamic regimes (temperature and species oscillations) not experimentally detected.

The agreement between experimental and numerical profiles is worse for the pyrolytic conditions. All the models predict no significant NH_3 conversion for the investigate temperatures and only "Nakamura" mechanism provides very low H_2 and N_2 concentrations for $T_{in} > 1200$ K. These results highlight that kinetic schemes are not satisfactorily tuned to describe ammonia pyrolysis and, perhaps, this aspect could affect also the prediction of the main features of ammonia oxidation. Further efforts are necessary to update the reaction chemistry set for a better understanding of ammonia chemistry.

Given this framework, this work aims a collecting new experimental data relative to ammonia oxidation and pyrolysis for promoting model tuning activities.

CRediT authorship contribution statement

Maria Virginia Manna: Conceptualization, Investigation, Formal analysis, Data curation, Writing - original draft. **Pino Sabia:** Conceptualization, Data curation, Methodology, Investigation, Writing - original draft. **Raffaele Ragucci:** Supervision, Writing - review & editing. **Mara de Joannon:** Conceptualization, Supervision, Writing - review & editing.

Declaration of Competing Interest

The authors declare that they have no known competing financial interests or personal relationships that could have appeared to influence the work reported in this paper.

Acknowledgements

This article is based upon work from COST Action SMARTCATs (CM1404), supported by COST (European Cooperation in Science and Technology, http://www.cost.eu).

Appendix A. Supplementary data

Supplementary data to this article can be found online at https://doi.org/10.1016/j.fuel.2019.116768.

References

[1] International Energy Agency. World Energy Outlook 2018, < https://www.iea.org/weo2018/ > ; 2018 [accessed 22.10.19].
[2] Moriarty P, Honnery D. Intermittent renewable energy: the only future source of hydrogen? Int J Hydrogen Energy 2007;32:1616–24.
[3] Chatzivasileiadi A, Ampatzi E, Knight I. Characteristics of electrical energy storage technologies and their applications in buildings. Renewable Sustainable Energy Rev 2013;25:814–30.
[4] Revankar ST. Chemical energy storage. In: Brinda H, Revankar S, editors. Storage and Hybridization of Nuclear Energy. Academic Press; 2019. p. 177–227.
[5] de Joannon M, Sabia P, Skevis G. Introduction of the special issue on SMARTCATs COST action. Energy Fuel 2018;32:10051.
[6] Ritter JA, Ebner AD, Wang J, Zidan R. Implementing a hydrogen economy. Mater Today 2013;6:18–23.
[7] Valera-Medina A, Xiao H, Owen-Jones M, David WIF, Bowen PJ. Ammonia for power. Prog Energy Combust 2018;69:63–102.
[8] Herbinet O, Dayma G. Jet-stirred reactors. In: Battin-Leclerc F, Simmie J, Blurock E, editors. Cleaner combustion. Green Energy and Technology. London: Springer; 2013. p. 183–210.
[9] Glarborg P, Dam-Johansen K, Miller JA, Kee RJ, Coltrin ME. Modeling the thermal DENOx process in flow reactors. Surface effects and nitrous oxide formation. Int J Chem Kinet 1994;26:421–36.
[10] Hinshelwood CN, Burk RE. The thermal decomposition of ammonia upon various surfaces. J Chem Soc 1925;127:1105.
[11] Roenigk KF, Jensen KF. Low pressure CVD of silicon nitride. J Electrochem Soc 1987;134:1777.
[12] Cooper DA, Ljungstrom EB. Decomposition of ammonia over quartz sand at 840–960 degree. Energy Fuels 1988;2:716.
[13] Busca G, Lietti L, Ramis G, Berti F. Chemical and mechanistic aspects of the selective catalytic reduction of NOx by ammonia over oxide catalysts: a review. Appl Catal B-Environ 1998;18:1–36.
[14] Rahinov I, Ditzian N, Goldman A, Cheskis S. NH_2 radical formation by ammonia pyrolysis in a temperature range of 800–1000 K. Appl Phys B 2003;77:541–6.
[15] Tsyganenko AA, Pozdnyakov DV, Filimonov VN. Infrared study of surface species arising from ammonia adsorption on oxide surfaces. J Mol Struct 1975;29:299–318.
[16] Hulgaard T, Dam-Johansen K. Homogeneous nitrous oxide formation and destruction under combustion conditions. AIChE J 1993;39:1342–54.
[17] Lyon RK, Benn DJ. Kinetics of the NO-O_2-NH_3 reaction. Proc Combust Inst 1978;17:601–10.
[18] Kijlstra WS, Daamen JC, van de Graaf JM, van der Linden B, Poels EK, Bliek A. Inhibiting and deactivating effects of water on the selective catalytic reduction of nitric oxide with ammonia over $MnOx/Al_2O_3$. Appl Catal B-Environ 1996;7:337–57.

[19] Turco M, Lisi L, Pirone R, Ciambelli P. Effect of water on the kinetics of nitric oxide reduction over a high-surface-area V_2O_5/TiO_2 catalyst. Appl Catal B-Environ 1994;3:133–49.
[20] Kusakabe K, Kashima M, Morooka S, Kato Y. Rate of reduction of nitric oxide with ammonia on coke catalysts activated with sulphuric acid. Fuel 1988;67:714–8.
[21] Lubrano Lavadera M, Sabia P, de Joannon M, Cavaliere A, Ragucci R. Propane oxidation in a Jet Stirred Flow Reactor. The effect of H_2O as diluent species. Exp Therm Fluid Sci 2018;95:35–43.
[22] Levenspiel O. Chemical Reaction Engineering. 3rd ed. New York: John Wiley & Sons; 1999.
[23] CHEMKIN-PRO 15131, Reaction Design: San Diego; 2013.
[24] Konnov AA, De Ruyck J. Kinetic modeling of the thermal decomposition of ammonia. Combust Sci Technol 2000;152:23–37.
[25] Glarborg P, Miller JA, Ruscic B, Klippenstein SJ. Modeling nitrogen chemistry in combustion. Progr Energy Combust Sci 2018;67:31–68.
[26] Song Y, Hashemi H, Christensen JM, Zou C, Marshall P, Glarborg P. Ammonia oxidation at high pressure and intermediate temperatures. Fuel 2016;181:358–65.
[27] Nakamura H, Hasegawa S, Tezuka T. Kinetic modeling of ammonia/air weak flames in a micro flow reactor with a controlled temperature profile. Combust Flame 2017;185:16–27.
[28] Klippenstein SJ, Harding LB, Glarborg P, Miller JA. The role of NNH in NO formation and control. Combust Flame 2011;158:774–89.
[29] Sabia P, Lubrano Lavadera M, Giudicianni P, Sorrentino G, Ragucci R, de Joannon M. CO_2 and H_2O effect on propane auto-ignition delay times under mild combustion operative conditions. Combust flame 2015;162:533–43.
[30] Monnery WD, Hawboldt KA, Pollock AE, Svrcek WY. Ammonia pyrolysis and oxidation in the Claus furnace. Ind Eng Chem Res 2001;40:144–51.
[31] Kobayashi H, Hayakawa A, Kunkuma KD, Somarathne A, Okafor EC. Science and technology of ammonia combustion. Proc Combust Inst 2019;37:109–33.
[32] Miller JA, Smooke MD, Green RM, Kee RJ. Kinetic modeling of the oxidation of ammonia in flames. Comb Sci Technol 1983;34:149–76.
[33] Mathieu O, Petersen EL. Experimental and modeling study on the high-temperature oxidation of Ammonia and related NOx chemistry. Combust Flame 2015;162:554–70.